Imaging

9

Roberto Pozzi Mucelli, Giovanni Foti and Luigi Romano

9.1 Introduction

Pancreatic neuroendocrine neoplasms (PanNENs) are a heterogeneous group of rare tumors of the pancreas originating from totipotential stem cells or differentiated mature endocrine cells within the exocrine gland. [1] Although rare, occurring in fewer than 1 in 100,000 people per year [2, 3], the frequency of PanNENs is progressively increasing as a result of better awareness by clinicians, radiologists, and pathologists [2].

These neoplasms usually occur sporadically but can occasionally be associated with genetic syndromes, such as multiple endocrine neoplasia type 1 (MEN1), von Hippel–Lindau disease, neurofibromatosis type 1, and tuberous sclerosis [4].

PanNENs produce and secrete hormones to a variable degree. When they produce symptoms related to excessive hormone production, the tumors are classified as syndromic or functioning pancreatic endocrine neoplasms (F-PanNENs) [5].

F-PanNENs are classified according to the name of the predominant hormone they secrete [5]. The two most common F-PanNENs are insulinoma and gastrinoma, followed by VIPoma, glucagonoma, somatostatinoma, and carcinoids [5].

In F-PanNENs, the role of imaging is mainly to detect the tumor [6, 7], which is usually quite small at diagnosis. Imaging also verifies lesion number and location and determines the exact location of the neoplasm, within and/or outside of the pancreas (in tumors with ectopic locations).

R. Pozzi Mucelli (✉)
Department of Pathology and Diagnostics, Radiology Unit, "G.B. Rossi" University Hospital, Verona, Italy
e-mail: roberto.pozzimucelli@univr.it

P. Pederzoli and C. Bassi (eds.), *Uncommon Pancreatic Neoplasms*, Updates in Surgery
DOI: 10.1007/978-88-470-2673-5_9, © Springer-Verlag Italia 2013

Non-functioning pancreatic endocrine neoplasms (NF-PanNENs) comprise about two-thirds of PanNENs (range: 10–48%), and more than half of all NF-PanNENs are malignant [5, 8-13]. They tend to manifest late, as large masses causing compression symptoms, or may be detected incidentally in asymptomatic patients. The role of imaging studies is to characterize the tumor, differentiating it from other tumor entities and in particular from ductal adenocarcinoma. This is an important distinction because malignant NF-panNENs have a more favorable prognosis (5-year survival rate 40% vs. 3%–5% for adenocarcinoma) [11, 12].

As they are often malignant [14,] NF-PanNENs also require accurate staging and appropriate follow-up.

Multiple imaging techniques have been employed in the evaluation of PanNENs, including ultrasonography (US), computed tomography (CT), and magnetic resonance imaging (MRI). Here we describe the imaging techniques available for the assessment of these rare lesions, pointing out the specific features of each imaging tool.

Also, the typical and atypical imaging features and diagnostic strategies available for both F-PanNENs and NF-PanNENs are analyzed.

9.2 Ultrasound

9.2.1 Imaging Technique

Trans-abdominal US represents a low cost, widely available imaging tool for evaluating PanNENs [15]. However, it does not allow lesion characterization, and correct interpretation of imaging strictly depends on the expertise and skills of the radiologist performing these procedures. Such limitations obviously become significant only in cases in which the pancreatic lesion is small or when an appropriate differential diagnosis is needed.

Also, trans-abdominal US may be diagnostically limited if either the patient's body habitus or gas in the bowel prevents a complete examination of the pancreas [16].

Recently published studies have shown that contrast-enhanced ultrasound (CEUS) can improve the identification of small F-PanNENs and the characterization of NF-PanNENs [17-20]. The intravenously injected contrast material (Sonovue, Bracco, Milan, Italy), together with the possibility to continuously visualize the lesion, allows a dedicated study to be performed, with depiction of the typical hypervascular enhancement pattern shown by the majority of PanNENs [17-20].

Endoscopic ultrasound (EUS) of the pancreas uses a high-frequency probe to generate images of the various regions of the pancreas [21]. Also, if a mass is present, biopsies can be performed through a conventional endoscope [22]. Patients undergoing EUS should fast starting at midnight of the night before the procedure. Intravenous access is established, and the patient is sedated.

After a preliminary endoscopic examination of the upper gastrointestinal tract, an endo-sonographic scope with a water-filled balloon in place is advanced as far into the duodenum as possible, and the duodenum, ampulla, and pancreas are visualized. Difficulty can be encountered if peristalsis is excessive or because of poor patient compliance.

Intraoperative ultrasound (IOUS) takes advantage of the direct placement of the US probe very close to the area of interest. Thus, because of the short distance of the probe to the target, e.g., the pancreas, a high-frequency transducer (7.5 or 10 MHz) can be used, yielding images with greater spatial resolution [23].

During IOUS of the exposed pancreas, the head of the gland is mobilized and the lesser sac is opened. The peritoneal cavity can be filled with warm saline. The transducer is enclosed in a sterile sheath and the pancreas is evaluated along its transverse and longitudinal planes, which permits visualization of both deep and superficial lesions [23, 24]. IOUS can be used to confirm the location of lesions identified preoperatively and to detect small lesions missed on other imaging studies.

9.2.2 Imaging Findings

Commonly, at trans-abdominal US the texture of the pancreatic gland can be considered as comparable to that of the liver. Pancreatic parenchyma is usually relatively hypoechoic in younger patients. An increase of fibrous and/or fatty tissues within the pancreas is usually associated with a relative increase in echogenicity compared to normal liver.

When detectable, small PanNENs (either functioning or non-functioning) appear as well-circumscribed nodules embedded in the pancreatic gland. These lesions are clearly hypoechoic compared to the normal pancreatic parenchyma [15, 17]. The majority of small lesions, measuring < 3 cm in diameter, are usually quite homogeneous on unenhanced US [17]. Small isoechoic lesions represent an important limitation for this imaging tool since they are frequently missed, especially in younger patients, because of the relatively hypoechoic appearance of the normal gland (Fig 9.1c).

At CEUS, PanNENs typically show early intense enhancement, indicative of hypervascular oval-shaped nodules distinct from the surrounding tissues (Fig. 9.1b, d) [17-20, 25].

Trans-abdominal US usually permits the correct identification of large PanNENs. The majority of these tumors appear as inhomogeneous hypo-/isoechoic masses relative to the normal pancreatic and liver parenchyma (Fig. 9.2) [25]. Most NF-PanNENs are large at presentation, with a well-defined multilobulated border and a compressive rather than an infiltrative pattern of growth [20, 25].

NF-PanNENs cannot be reliably characterized using conventional US. (Figs. 9.1, 9.2); however, once they are detected on baseline scan, CEUS

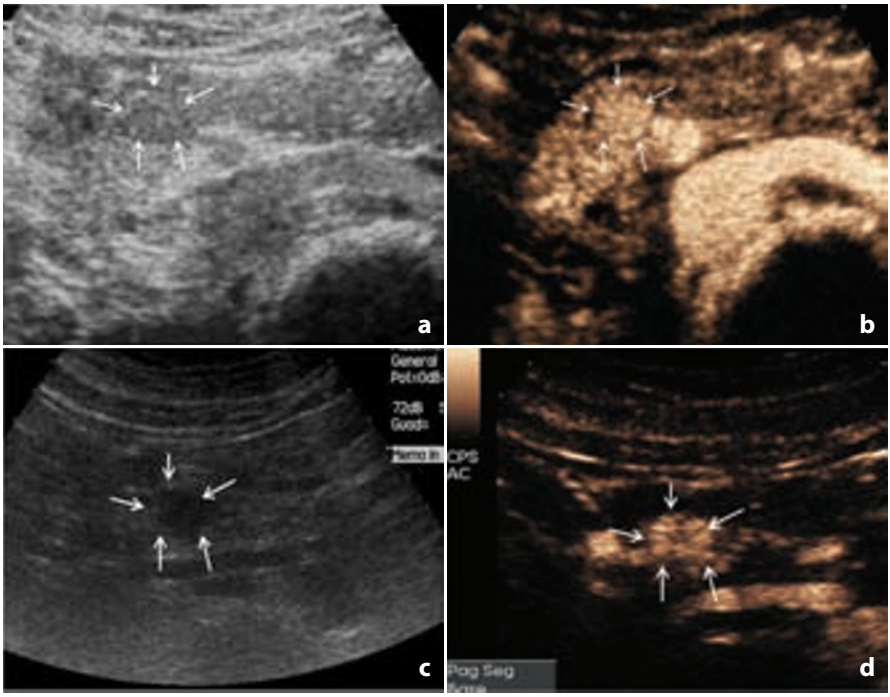

Fig. 9.1 Trans-abdominal US and CEUS imaging findings of small PanNENs. Small iso-echoic tumor (*arrows*) located on the pancreatic head (**a**), showing early intense enhancement (*arrows*) on CEUS (**b**). Typical small hypoechoic insulinoma of the pancreatic head (*arrows* in **c**), seen as a hypervascular focal lesion (*arrows*); for comparison, normal parenchyma as seen on CEUS (**d**)

allows for their dynamic evaluation and characterization. The early and intense enhancement and the slow washout of hypervascularized tumors can be documented (Figs. 9.1, 9.2) and is a key feature in the differential diagnosis with adenocarcinoma, which usually appears as a hypovascular mass [20, 25].

Small lesions, measuring < 3 cm in diameter, usually enhance homogenously [17].

Intralesional necrosis and or hemorrhagic areas, frequently encountered in large lesions, result in inhomogeneous central hypoechoic areas better depicted at CEUS [15, 20, 25].

Large lesions may be associated with the encasement of arterial or venous vessels and with peri-tumoral lymphadenopathy.

Metastatic disease in the liver occurs in about 30% of cases [13, 25] and represents a clear sign of malignancy. The US appearance of the liver metastases is variable. Hyperechoic nodules or a target-like appearances at baseline

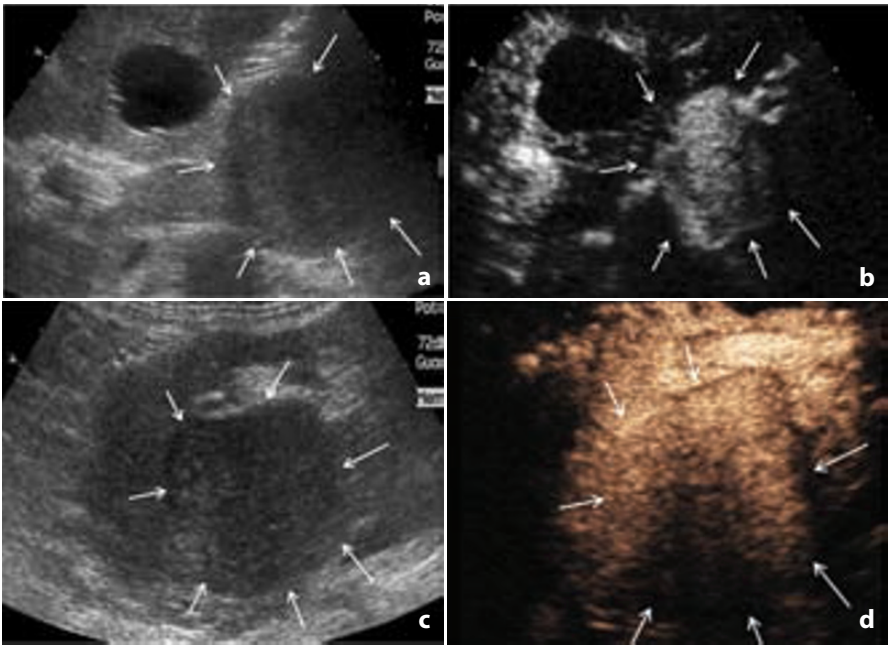

Fig. 9.2 Trans-abdominal US and CEUS imaging findings of NF-PanNENs. A large hypoechoic tumor (*arrows*) located on the pancreatic body (**a**), showing early intense enhancement (*arrows*) on CEUS (**b**). Large well-defined hypoechoic NF-PanNEN of the pancreatic head (*arrows* in **c**), seen as a hypervascular focal lesion (*arrows*) at CEUS (**d**)

US suggests an endocrine nature of the primary tumor, but this pattern is not specific. In other cases, the metastases show a non-specific hypoechoic pattern [15, 25]. A dedicated CEUS study of a suspected liver lesion may point out the typical hypervascularity shown by endocrine tumors during their early dynamic study (Fig. 9.3).

EUS visualizes islet-cell tumors as a relatively hypoechoic area compared with the adjacent pancreas, with smooth and at times slightly irregular margins that are well demarcated.

In the identification of small lesions located in the pancreatic head, EUS has high sensitivity but it may be limited in completely evaluating the tail of the pancreas, depending on its location [26]. A recently published study demonstrated the value of EUS in the preoperative assessment of patients with MEN1 [27].

In the identification of small F-PanNENs during surgery, a combination of intraoperative palpation and IOUS was found to achieve the best results due to the complementary nature of these two techniques.

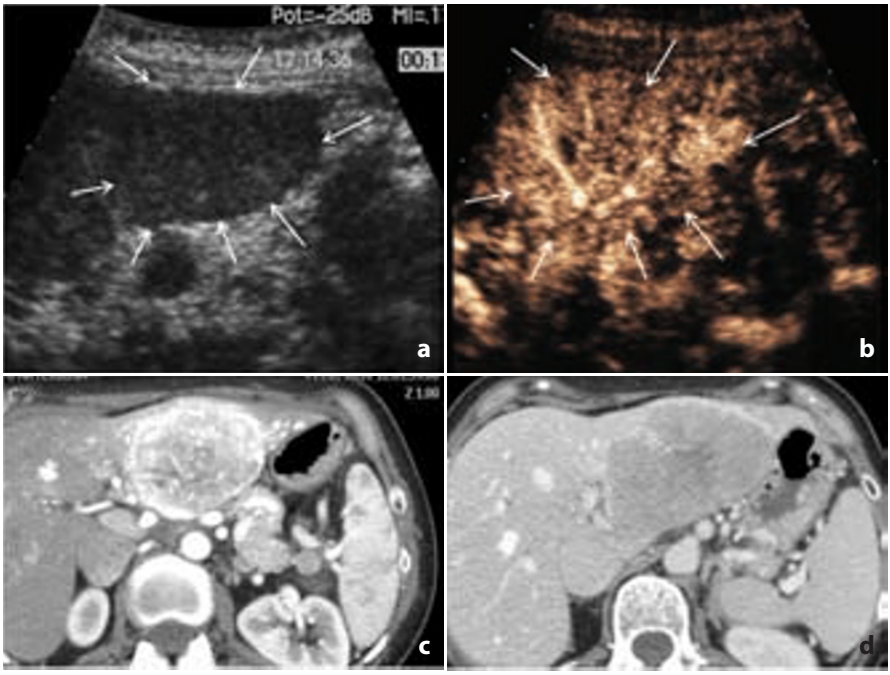

Fig. 9.3 Large liver metastasis from a NF-PanNEN/C studied using trans-abdominal US and CEUS and MDCT. A large, slightly hypoechoic, focal liver lesion (*arrows*) can be appreciated in the left lobe (**a**). The lesion shows early intense enhancement (*arrows*) on CEUS (**b**). At MDCT, during arterial pancreatic phase (**c**), the lesion has the typical hypervascular pattern of endocrine tumors, with subsequent washout during portal venous phase (**d**)

9.3 Computed Tomography

9.3.1 Imaging Technique

Multidetector computed tomography (MDCT) is a widely available imaging technique capable of providing, in a short examination time, images characterized by excellent spatial and contrast resolution. The MDCT protocol should include both unenhanced and enhanced scans, as the former, obtained at baseline, can be useful in the detection of intralesional calcifications (which may occur in F- and NF-PanNENs) (Fig. 9.4), and to accurately plan the dynamic contrast-enhanced study.

The intravenous administration of iodinated contrast agent is needed to optimally visualize the pancreatic parenchyma, increasing contrast resolution [28].

PanNENs are frequently hypervascular focal lesions, appearing as high-attenuating lesions during early contrast-enhancement phases [29, 30] (Figs. 9.5, 9.6). Accordingly, the protocol should include at least two contrast-enhanced phases

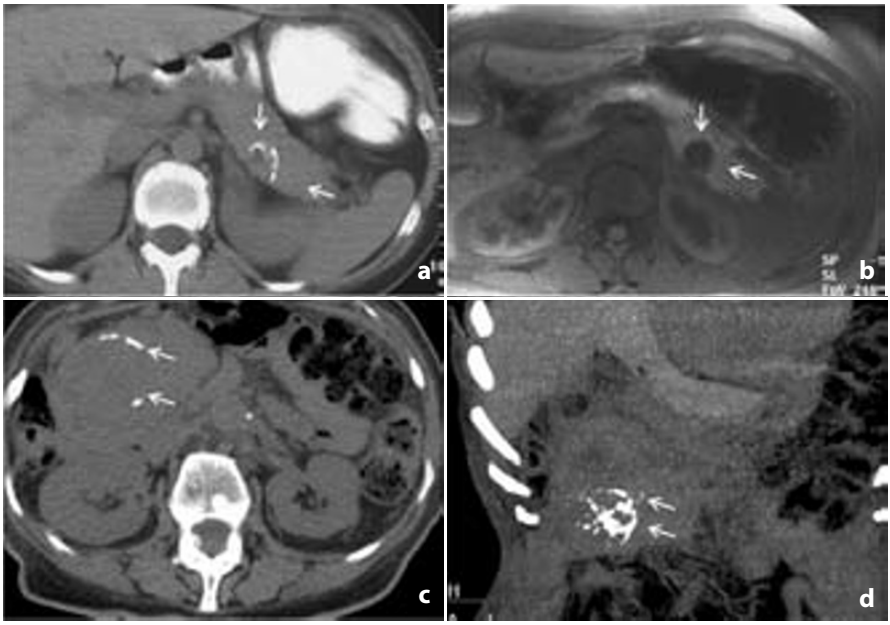

Fig. 9.4 Calcification in PanNENs. Unenhanced CT scan points out a tiny F-PanNEN located in the pancreatic tail, with intralesional calcifications (**a**). These are not depicted on T1-weighted MRI (**b**). A large NF-PanNEN located in the pancreatic head, with intralesional calcifications depicted on unenhanced axial (**c**) and coronal (**d**) scans

[30-32], acquired, respectively, with a 40- to 45-s delay (arterial pancreatic phase) and a 70- to 80-s delay (portal venous phase) after the administration of contrast material (calculated by using the bolus-tracking technique).

However, about 30% of these tumors will have an atypical vascular pattern, resulting in iso- or even hypoattenuating lesions with respect to adjacent pancreatic parenchyma (Fig. 9.7) [13].

In our experience, in most cases the best enhancement is obtained during the arterial pancreatic phase [13]; nonetheless, additional contrast-enhanced scans should be taken in selected cases. An early arterial phase, acquired with a delay of 20–25 s (vascular arterial phase), may be useful in the detection of small tumors characterized by subtle brief enhancement. In addition, it may allow detailed arterial vascular mapping, which is useful for staging locally advanced tumors and for treatment planning (Fig. 9.8).

A late venous phase, acquired with a delay of about 120 s, may be useful for depicting a delayed hypervascular enhancing pattern. A multi-phase imaging protocol therefore offers the advantage of increasing the possibility of demonstrating the typical hypervascular pattern of PanNENs, to allow locoregional staging and the detection of liver metastases [13].

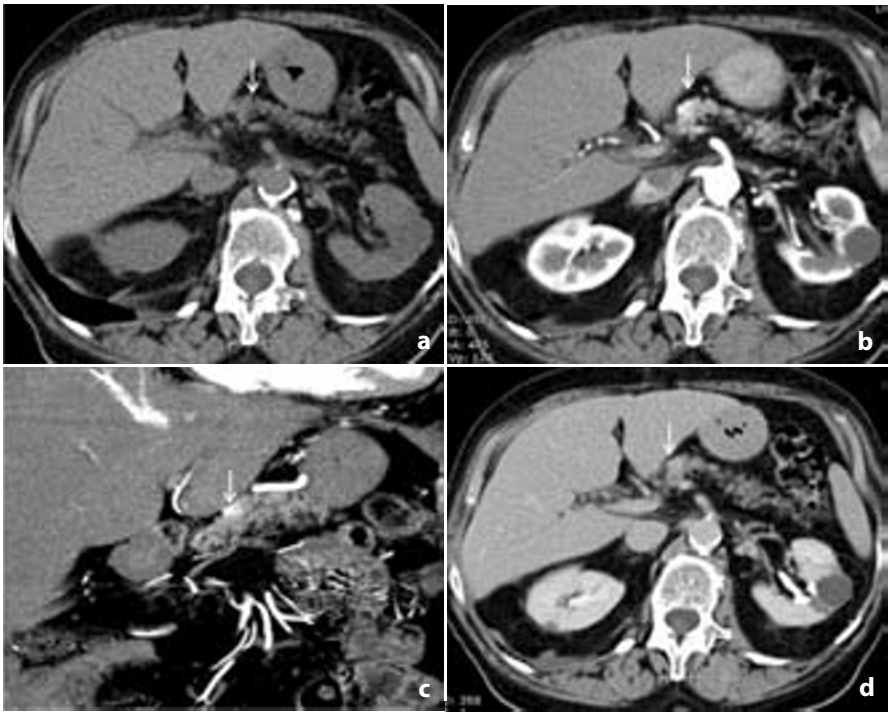

Fig. 9.5 Typical tiny insulinoma studied by MDCT. The lesion (*arrow*) appears isodense on baseline unenhanced scan (**a**). During a contrast-enhanced study, the lesion (*arrow*) shows the typical hyperdensity on axial (**b**) and para-coronal reconstructed images obtained from the arterial pancreatic phase (**c**), showing washout during the venous phase (**d**)

Curvilinear reconstructions should be used to highlight the relationship between primary tumors and the pancreatic and biliary ductal systems (Fig. 9.9).

The patient can be administered a glass of water immediately before the examination, to assure optimal filling of the stomach and duodenum with a low-contrast medium and for better definition of the gastric and duodenal wall. We usually avoid administrating oral iodinated contrast material, to avoid the misinterpretation or masking of hypervascular lesions ectopically located within the duodenal or small-bowel wall.

9.3.2 Imaging Findings

Baseline CT usually depicts PanNENs as isodense masses with respect to normal parenchyma (Figs. 9.5a, 6a, 7a). Thus, the tumor might be missed on an unenhanced scan, unless it has a large diameter and/or is associated with a distorted morphology of the gland [13].

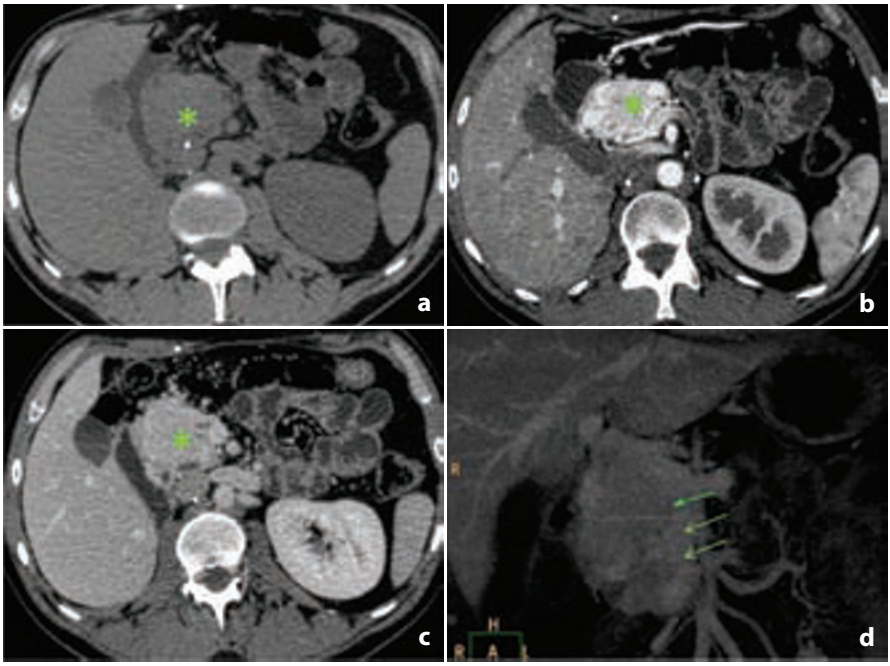

Fig. 9.6 Typical enhancement pattern of NF-PanNEN/Cs studied by MDCT. The lesion (*star*) appears isodense on baseline unenhanced scan (**a**). During contrast-enhanced study, the tumor (*star*) shows the typical hyperdensity on axial images obtained during arterial pancreatic (**b**) and portal venous phases (**c**). Para-coronal reconstructed images obtained during the portal venous phase better depicts encasement of the superior mesenteric vein (*arrows* in **d**)

Tumor inhomogeneity may be caused by globular or lamellar calcifications, seen both in F-panNENs (mostly insulinomas) and in NF-PanNENs, in these cases often associated with large areas of necrosis (Fig. 9.4a, b, d) [33].

During dynamic contrast-enhanced study, both functioning and non-functioning PanNENs usually appear as well-defined round or oval-shaped hypervascular masses [33]. At MDCT, the most frequent peak-enhancement phase is the arterial pancreatic phase whereas rapid washout is frequently seen in the portal venous and late venous phases (Fig. 9.6).

Achieving an intense enhancement is also useful to better define the dimensions of the tumors and to evaluate the relationship with adjacent structures [34] (Fig. 9.10).

Enhancement is usually homogeneous in small lesions, measuring < 3 cm in diameter [13, 33]. Conversely, large tumors, measuring > 3 cm in diameter, are typically inhomogeneous because of the presence of intralesional necrotic areas or cystic degeneration [13, 35], appearing as hypodense areas compared with the viable hypervascularized neoplastic tissue (Fig. 9.9).

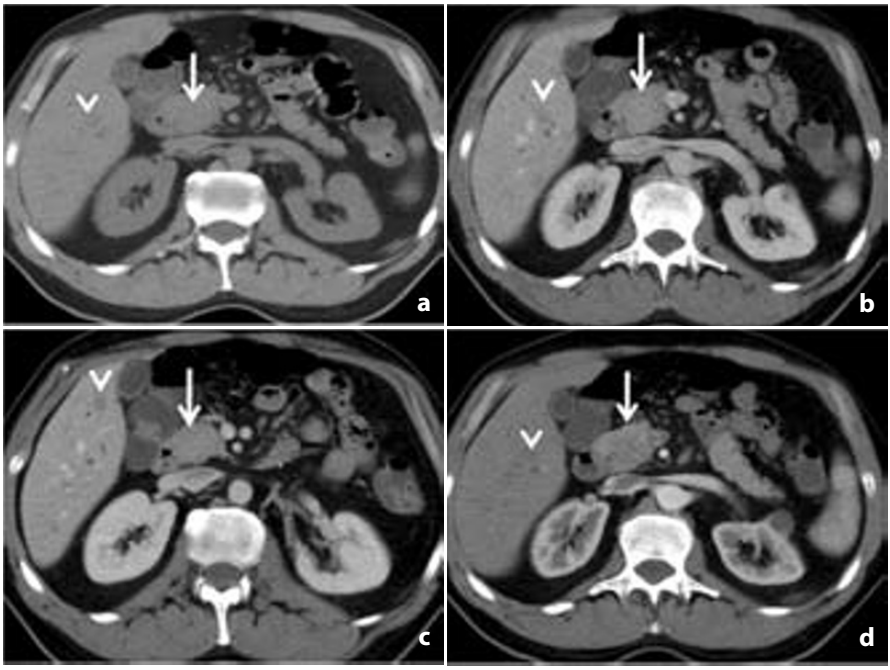

Fig. 9.7 Atypical enhancement pattern of PanNEN/Cs studied by MDCT. The lesion (*arrow*) appears isodense on baseline unenhanced scan (**a**). During contrast-enhanced study, the tumor (*arrow*) is isodense on axial images obtained during arterial pancreatic (**b**) and portal venous phases (**c**, **d**). Multiple, tiny, slightly hypodense liver metastases are seen in segments V and VI (*arrowhead*)

MDCT, due to its high spatial, contrast, and temporal resolution, is advantageous in loco-regional staging, depicting the encasement of both the arterial (superior mesenteric artery or the celiac axis) and venous (superior mesenteric vein and portal vein) vessels [13, 33]. Three-dimensional reconstruction of the peri-pancreatic vessels may be of help in treatment planning (Fig 9.8).

Neoplastic thrombus within the peri-pancreatic veins has the same density as the mass from which it derives, thus displaying a slightly lower density than the vascular lumen.

Secondary phenomena, such as bile duct dilation or vascular encasement, may be well-demonstrated by means of MDCT, using axial native images and multi-planar dedicated reconstructions (Fig. 9.9b) [13]. Also, dilatation of the biliary tree may be depicted in case of tumors located in the pancreatic head.

Depending on its location, the primary tumor may dislocate or compress adjacent structures such as the stomach and duodenum, spleen and left kidney, and the adrenal gland (Fig. 9.11). Frank invasion into adjacent viscera is rare and is usually associated with the presence of an endocrine carcinoma.

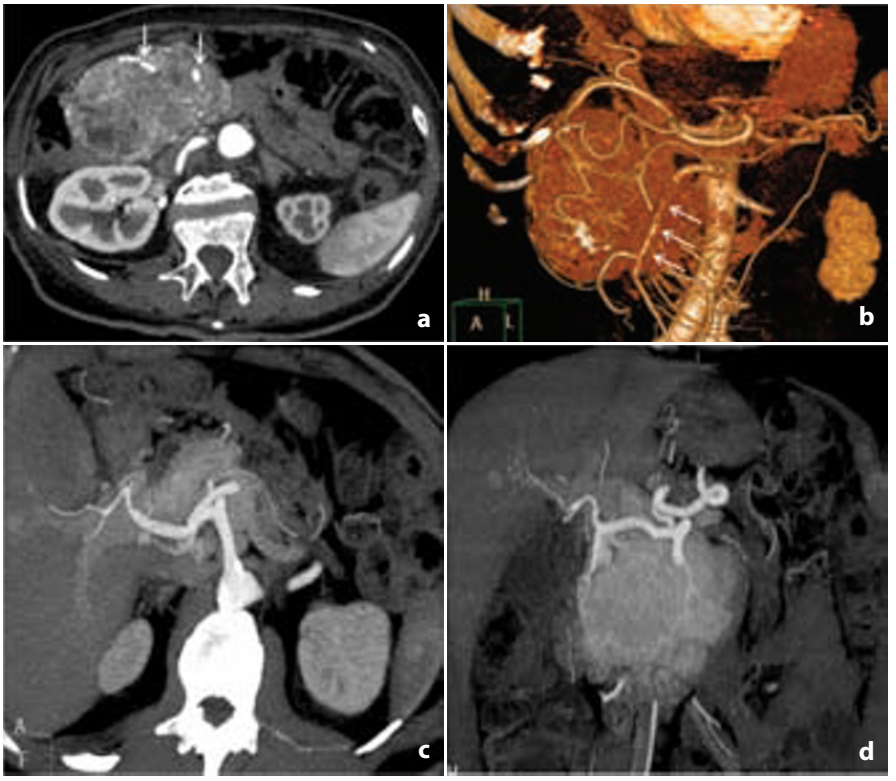

Fig. 9.8 Vascular encasement demonstrated using MDCT reconstructions. A large inhomogeneous NF-PanNEN/C of the pancreatic head is associated with complete encasement of multiple vessels (*arrows*), depicted on axial images. The volume-rendering reconstructed image obtained from the arterial pancreatic dataset (**b**) clearly shows the encasement of multiple vessels, including the superior mesenteric artery (*arrows*). Maximum-intensity projection (MIP) reconstructions (**c, d**) in another patient show involvement of the celiac axis

Even if less accurate than MRI in identifying liver metastases, MDCT represents a reliable tool for the identification of metastatic involvement of the liver in case of PanNENs [13, 33].

There is no difference between the metastases of F-PanNENs and NF-PanNENs. These lesions usually share imaging features of primary tumors, i.e., slightly hypodense compared with the normal parenchyma on unenhanced CT scan, and hyperdense hypervascular lesions (sometimes with a target-like pattern) on arterial enhanced scan [30, 36]. Liver metastases typically show washout during portal venous and late venous phases, resulting in lesions hypodense to normal liver parenchyma (Fig. 9.3c, d). Calcifications may be present as well.

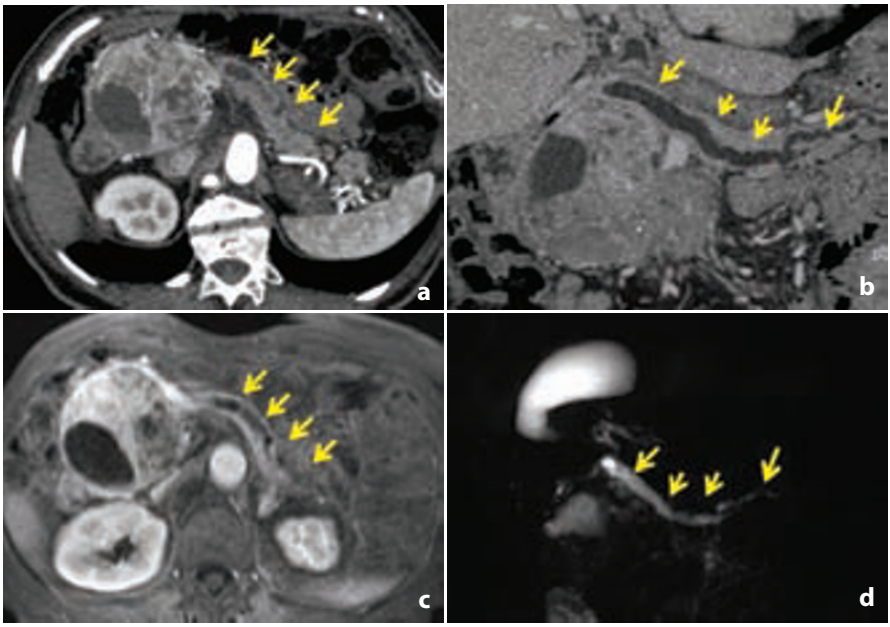

Fig. 9.9 Involvement of the main pancreatic duct, demonstrated using MDCT and MRI. A large inhomogeneous NF-PanNEN/C of the pancreatic head is associated with the complete upstream dilatation of the main pancreatic duct (*arrows* in **a**). The dilatation is better depicted using curvilinear reconstruction in the para-coronal plane (**b**). Dilatation of the main pancreatic duct (*arrows*) is well-depicted using contrast enhanced MRI, as seen on the axial plane (**c**) and on the MRCP image (**d**)

Hypovascular liver metastases may be associated with hypovascular primary tumors (Fig. 9.7).

The typical features of NF-PanNENs, such as a well-demarcated hypervascular mass with a compressive pattern of growth, are present in about 70% of patients [13, 15, 28, 33]. In the other 30%, the pattern is non-specific and a reliable differential diagnosis with ductal adenocarcinoma is not possible [37], since the tumor is mainly hypodense compared with the pancreatic parenchyma (Fig. 9.7).

When the mass is large and well-circumscribed, a ductal adenocarcinoma can be excluded, but the problem of differential diagnosis from other rare, solid tumors remains, including solid variants of micro-cystic cystadenoma and pancreatic metastases.

PanNENs may appear as iso-attenuating to normal pancreas in pancreatic phase CT images, and sometimes are better delineated in the portal venous phase [13, 38]. Late enhancement of the tumor may be explained by extensive necrosis, resulting in a slower washout from the mass, due to the reduced vascularization [39].

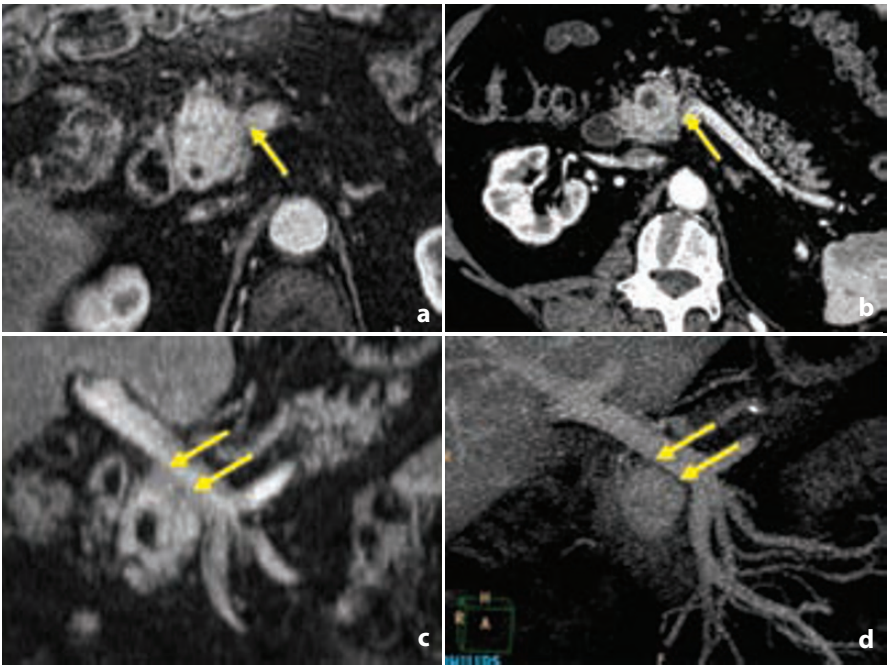

Fig. 9.10 Involvement of peri-tumoral vessels, assessed using MDCT and MRI. A relatively small but inhomogeneous NF-PanNEN/C of the pancreatic head is located close to the superior mesenteric vein (*arrow*) on axial portal-enhanced MRI (**a**) and MDCT (**b**). Coronal reconstructions obtained using MRI (**c**) do not rule out vessel, involvement (*arrows*). Conversely, MDCT (**d**), with its higher spatial resolution, demonstrates the presence of an adipose interface between tumor and vessel (*arrows*)

9.4 Magnetic Resonance Imaging

9.4.1 Imaging Technique

In patients with PanNENs, the information obtained with MRI is similar to that obtained with CT, with the additional advantage that the patient is spared radiation exposure. However, due to its relatively limited availability and the longer examination time, MRI is not as widely used as CT for imaging pancreatic tumors.

State-of-the-art MRI of pancreatic neoplasms is optimally performed with 1.5 Tesla gradient systems using phased-array coils to improve the signal-to-noise ratio, optimized with thin slices and a small field of view [13, 40]. Breath-hold acquisitions are obtained with fast spin echo (FSE) or gradient echo (GRE) sequences and echo planar imaging. A moderately T2-weighted FSE and single-shot FSE (SSFSE) should be obtained, followed by T1-weighted in-phase GRE and T1-weighted opposed-phase GRE.

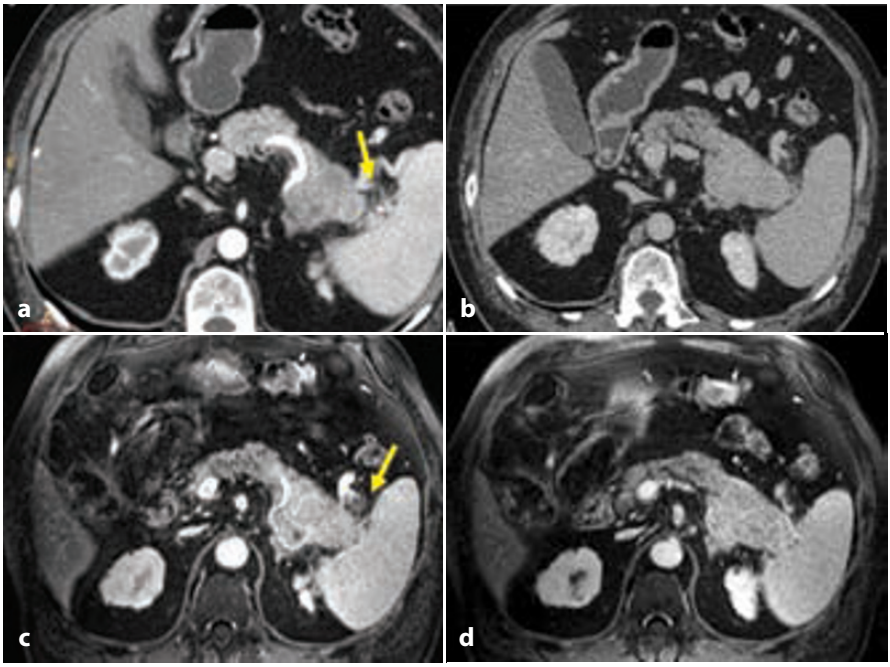

Fig. 9.11 Infiltration of adjacent structures as assessed using MDCT (**a**, **b**) and MRI (**c**, **d**). A large inhomogeneous NF-PanNEN/C of the pancreatic tail infiltrates the splenic hilum and peri-pancreatic fat (*arrow*), as well-depicted with both modalities

T1-weighted images with fat suppression have proven to be useful for imaging the pancreatic gland, allowing high contrast resolution between the normal bright parenchyma and the surrounding hypointense retroperitoneal fat [41]. Coronal and axial magnetic resonance cholangiopancreatography (MRCP) with SSFSE accurately depicts the pancreatic ducts.

For the evaluation of PanNENs, fat-suppressed three-dimensional spoiled GRE sequences after the administration of gadolinium-DTPA are acquired in arterial phase (30–40 s), portal phase (70–80 s), and equilibrium phase (180 s) [13, 40, 41]. The acquired images should cover the upper abdomen, including the entire liver, thus improving the detection and characterization of loco-regional lymph-nodes and hepatic lesions [13].

Similar to contrast-enhanced helical CT, additional gadolinium enhanced scans can be obtained in the early arterial (scan delay 20 s) or late venous (120 s) phases, which increases the possibility of imaging the typical hypervascular enhancement pattern of these tumors [13, 31, 42].

9.4.2 Imaging Findings

On T1-weighted images, the normal pancreas exhibits medium to high signal intensity, similar to or slightly less than that of liver, but lower than that of retroperitoneal fat.

Fat suppression should be used, especially for T1 sequences, to increase pancreatic conspicuity, since with this technique the pancreas assumes a bright signal intensity that facilitates the detection of focal lesions [41, 42]. In patients with fatty involution of the pancreas, the signal intensity of this organ increases on T1-weighted sequences according to the amount of fat present within the parenchyma. Consequently, the pancreatic bed appears as an area of very low signal intensity on fat-sat sequences, which therefore are of little use in the visualization of small tumors (Fig. 9.12).

T2-weighted images with fat suppression may be useful for the evaluation of peri-pancreatic structures and inflammatory changes, but they are not strictly needed for imaging panNENs. On TSE T2-weighted images, the pancreas

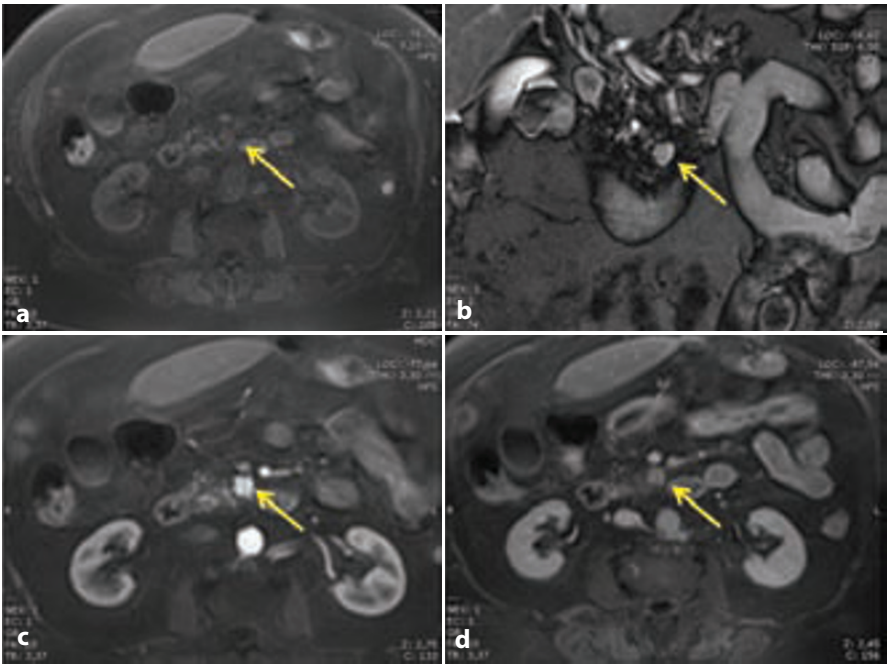

Fig. 9.12 Typical MRI finings of insulinoma. The on baseline unenhanced scan shows the lesion (*arrow*) as hypointense on the fat-saturated, T1-weighted, axial image (**a**) and hyperintense on the coronal T2-weighted image (**b**). During the contrast-enhanced study, the lesion (*arrow*) shows the typical hypervascularity on axial images obtained during the arterial pancreatic phase (**c**) and subsequent washout during late venous phase (**d**)

demonstrates intermediate signal intensity, similar to that of the liver. The signal may be intermediate to low on HASTE sequences.

The surface of the normal pancreatic parenchyma may be either smooth or lobulated.

Pancreatic ducts appear as low-signal intensity tubular structures on T1-weighted sequences and as high-signal intensity structures on heavily T2-weighted scans. At MRCP, heavy T2-weighting and fat suppression provide a cholangiogram useful for the evaluation of pancreatic and biliary duct involvement.

The typical MRI features of panNENs include a pancreatic mass of low signal intensity on T1-weighted images and of intermediate to high intensity on T2-weighted images (Fig. 9.12). As previously stated, the better intrinsic contrast resolution of this imaging technique may be advantageous for the identification of very small primary tumors, which frequently appear hypointense relative to the normal parenchyma on T1-weighted sequences. Lesion conspicuity is usually enhanced by fat-suppression.

Small lesions, which account for the majority of F-panNENs and some incidentally detected NF-PanNENs, are often quite homogeneous. Conversely, larger tumors may appear markedly inhomogeneous due to intralesional necrosis or hemorrhage, which may be seen as hyperintensity on T1-weighted images [43] and inhomogeneous hyperintensity on T2-weighted images (Fig. 9.13).

Cystic tumors have been described [35] and are often associated with widespread intralesional necrosis. Cystic lesions are usually unilocular, with contents that are hypointense on T1-weighted and hyperintense on T2-weighted images [44]. The cystic wall may show variable thickness [44]. The appearance of these tumors may be similar or even identical to that of other cystic tumors of the pancreas. Sometimes, intense enhancement of a peripheral ring-shaped viable tumor will suggest the diagnosis of cystic NF-panNENs (Fig. 9.14); however, in the majority of cases, a definitive diagnosis can only be obtained by histological examination of the resected specimen.

Among their atypical features, some islet tumors may have a low signal intensity on T2-weighted images due to the presence of abundant fibrous tissue [45]; in such cases they may be indistinguishable from ductal adenocarcinoma.

As seen for CT, during dynamic contrast-enhanced study, the majority of PanNENs show a typical hypervascularity [13, 31, 33, 46], resulting in hyperintense lesions compared to normal pancreatic and liver parenchyma (Figs. 9.11c, d, 9.12, 9.13).

In general, small tumors are depicted as homogeneously enhancing lesions (Fig. 9.12), whereas large tumors may appear markedly inhomogeneous during dynamic studies, since central necrotic areas remain hypointense on T1-weighted images even after contrast medium administration (Fig. 9.13).

The highest signal intensity is most frequently reached in the pancreatic phase [13] although the lesions may remain hyperintense during the portal

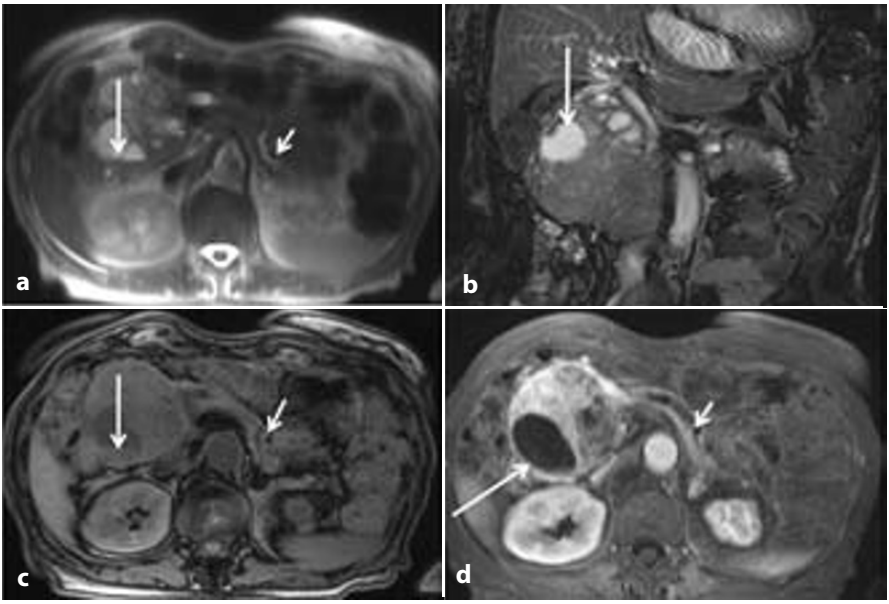

Fig. 9.13 Typical MRI findings of large NF-PanNEN/Cs. Pre-contrast examination shows a large tumor of the pancreatic head with upstream dilatation of the main pancreatic duct (*short arrow*). The lesion is markedly inhomogeneous on axial (**a**) and coronal (**b**) T2-weighted images and on the axial T1-weighted image, presenting intralesional necrosis and cystic changes with a fluid-fluid level (*long arrow*). After gadolinium administration (**d**), tumor inhomogeneity due to cystic change is confirmed (*long arrow*)

enhanced phase [30, 45]. Alternatively, some lesions may show early washout during the portal and late venous phases.

Persistent hyperintensity during late enhanced phases is found mainly in the larger lesions, where the neoplastic thrombosis of the draining veins results in retention of contrast medium [30].

The usefulness of delayed gadolinium-enhanced T1-weighted images (obtained 5–10 min following injection) has been postulated in scirrous tumors, showing delayed enhancement [31] (Fig. 9.15).

As for CT, the best dynamic phase for studying endocrine tumors is still a matter of debate; however, without any radiation exposure, modern fast breath-hold sequences should be used to obtain multiple contrast-enhanced phases during dynamic study, including early arterial, arterial pancreatic, portal venous, and late venous phases.

Multi-phasic dynamic study enhances the likelihood of detecting liver metastases, frequently imaged as hypervascular hepatic lesions [13, 36, 45] during the arterial pancreatic phase (Fig. 9.16). Metastases can also be depicted as hypovascular focal liver lesions during portal and late venous phases.

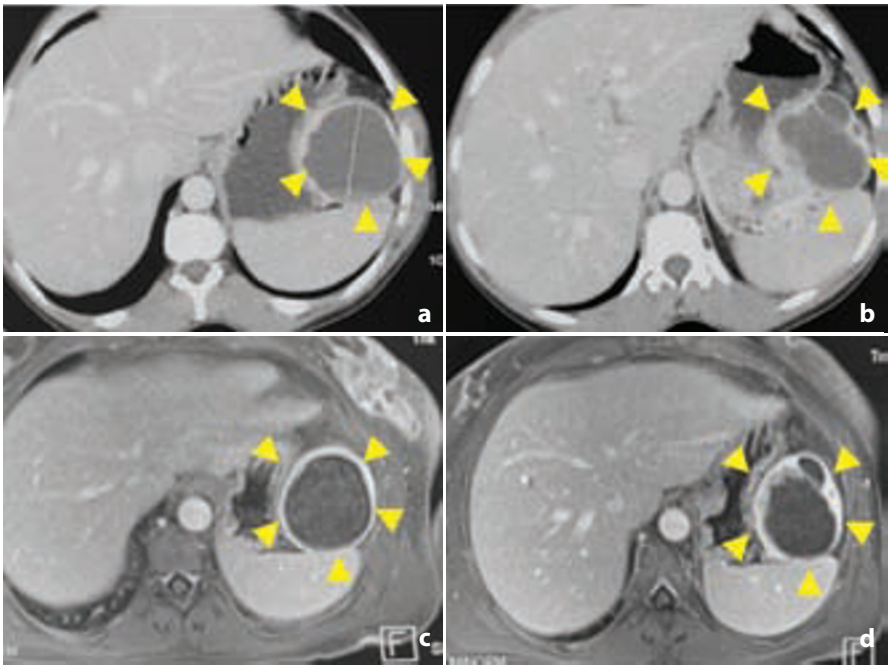

Fig. 9.14 Cystic PanNEN studied using MDCT and MRI. A large cystic PanNEN of the pancreatic tail can be recognized on the axial images acquired during portal venous phase, both at MDCT (**a**, **b**) and at MRI (**c**, **d**). The ring-shaped pattern of enhancement (*arrowheads*) is better depicted on the latter. A differential diagnosis with other cystic pancreatic tumors cannot be obtained in this case

The value of liver-specific Gd-chelates in the identification of both primary pancreatic tumor and hepatic metastases has been reported [47, 48]. Delayed hepato-biliary phase, obtained after the administration of liver-specific contrast material, can detect small metastases that other sequences may have failed to demonstrate [48].

9.5 Other Radiologic Diagnostic Tests

Before non-invasive cross-sectional imaging methods were introduced, selective arteriography of the proper or common hepatic artery, the gastroduodenal, splenic, superior mesenteric, and at times the dorsal pancreatic artery was the principal technique for localizing these hypervascular endocrine tumors of the pancreas. The arteriographic appearance of all islet cell tumors is similar for F-PanNENs and NF-PanNENs. It is not possible to distinguish a functioning from a non-functioning tumor or one type of functioning tumor from another. However, the marked hypervascularity and intense homogeneous staining permit

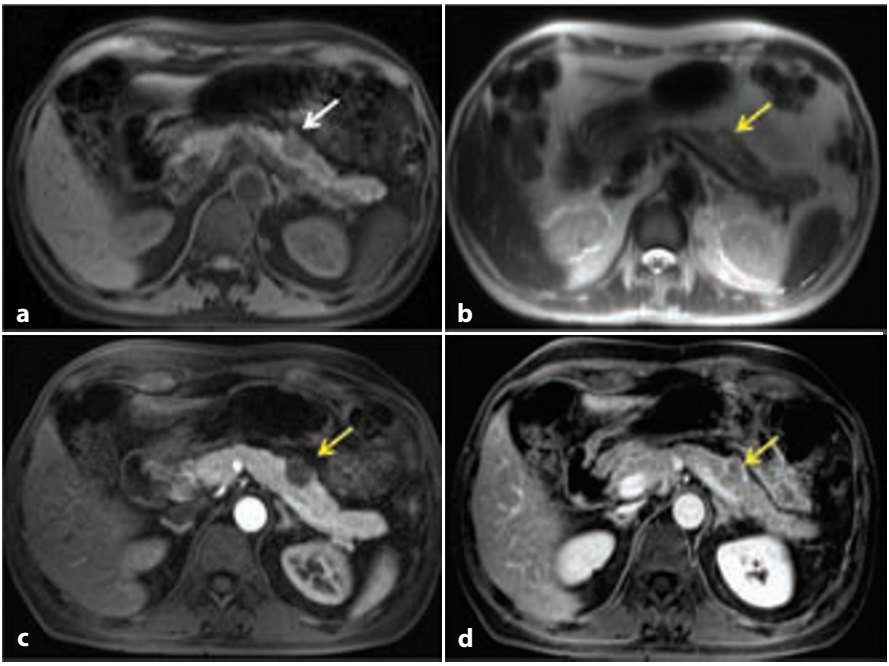

Fig. 9.15 Atypical delayed enhancement of a PanNEN of the pancreatic body. A relatively small NF-PanNEN is hypointense on the pre-contrast T1-weighted image (**a**) and slightly hyperintense on the T2-weighted image (**b**). The tumor is hypovascularized during the arterial pancreatic phase (**c**) but shows delayed enhancement, resulting in an isointense lesion with a thin hyperintense rim on the enhanced axial image acquired at the time of late venous phase (**d**)

the distinction of PanNENs from other tumors such as pancreatic adenocarcinoma [49]. Arterial and venous involvement can often be demonstrated in larger lesions.

Neovascularity and portal vein invasion indicate that the tumor is malignant.

Portal venous sampling (PVS), also called pancreatic venous sampling or trans-hepatic venous sampling, involves catheterization of the portal vein using a trans-hepatic approach [50]. The branches of the extrahepatic portal venous system are selectively catheterized and blood samples obtained. The sample with the highest concentration of tumor cells comes from the vein that drains the area of the tumor.

In case of arterial stimulation with venous sampling, the tumor is stimulated to secrete hormones by a specific injected secretagogue, and venous samples are obtained from the right and left hepatic veins [49] at 0.5, 1, and 2 min after each injection. If the hormone concentration increases, the arterial supply to the tumor can be identified and therefore the region where the tumor is located. If the hormone concentration increases after the drug has

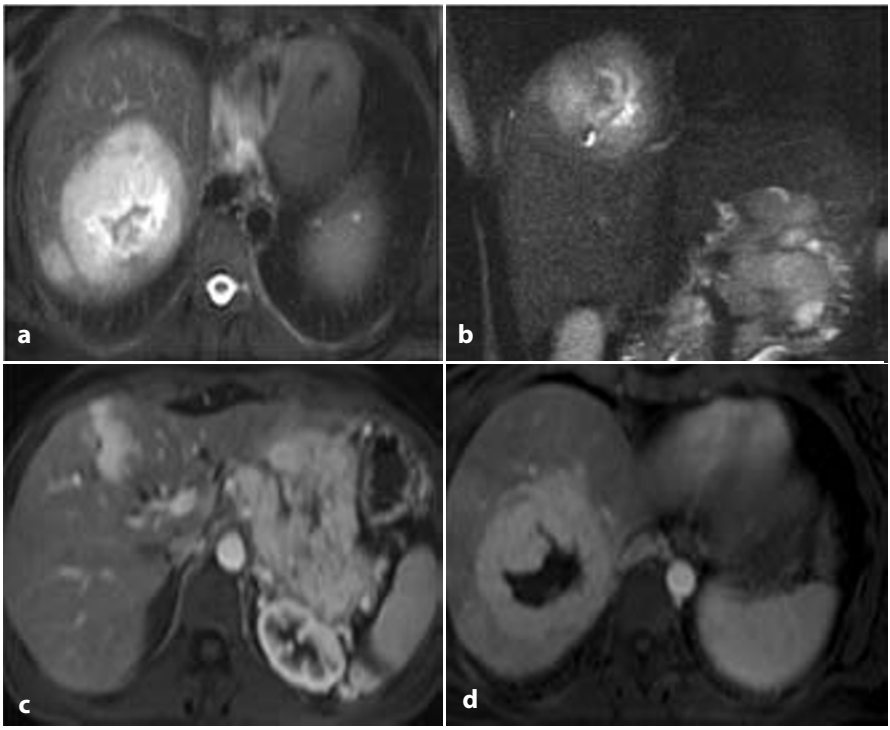

Fig. 9.16 Liver metastases studied using MRI. Large metastases appear homogeneously hyperintense on the T2-weighted image (**a**, **b**). Small metastases are hypervascular during arterial pancreatic phase (**c**), whereas a large lesion may show inhomogeneity due to central necrosis (**d**)

been injected into the proper hepatic artery, the presence of hepatic metastases can be diagnosed.

Based on the measurement of the hormone concentration in each venous sample, these diagnostic methods were employed in the past for evaluating functioning tumors. However, due to high cost and relative invasiveness, these tools are no longer used in clinical routine.

9.6 Imaging Features of Functioning F-PanNENs

Among the islet cell tumors of the pancreas, insulinoma is the most common endocrine tumor, followed by gastrinoma, VIPoma, glucagonoma, somatostatinoma, and other, rarely encountered pancreatic secretory tumors.

In functioning tumors, the clinical data and laboratory tests often permit an accurate clinical diagnosis, so that cross-sectional imaging is used to localize the tumor within or eventually outside the pancreas, guiding the surgeon to the appropriate tumor resection.

Patients suffering from MEN1 pose a radiologic challenge, because of the possibility of multiple pancreatic and extrapancreatic tumors (mainly located in the duodenal or gastric wall).

9.6.1 Insulinoma

Insulinomas are frequently small at detection, often measuring < 2 cm, at diagnosis due to the fact that symptoms related to hypoglycemia can occur even with small amounts of insulin.

Most insulinomas (90%) are benign solitary lesions; sporadic lesions are more frequently encountered in women (60%), especially between the fifth and sixth decades of life.

Malignancy should be suspected in case of large (> 2 cm) lesions or intralesional calcifications.

The appearance of liver metastases is similar to that of the primary tumor, i.e., hypervascular during arterial phases and showing washout during portal and late venous phases.

Patients suffering from MEN1 tend to present with multiple tumors, especially in case of presentation at a young age.

On abdominal US, when detectable according to their location and to patient habitus, insulinomas may appear as hypoechoic lesions compared to normal parenchyma; however, in many cases they are iso-echocic with respect to the surrounding parenchyma. In addition, due to their frequently small size, a mass effect cannot be considered as a reliable finding for lesion detection. When a tumor is visualized or suspected on the basis of a baseline scan, the intravenous administration of sonographic contrast material may help in its identification, as it typically appears at CEUS as a hypervascular focal lesion [17].

Endoscopic ultrasound provides excellent results for tumors in the head of the pancreas (sensitivity 83%) but poor sensitivity (38%) for those located in the tail [21].

On CT, these lesions are usually isodense to normal parenchyma on baseline scan. The presence of calcifications may help in the detection of a small lesion, especially in case of poorly enhancing lesions.

The majority of insulinomas appear as brightly enhancing, round to oval masses that demonstrate rapid washout in the portal and late venous phases [33]. Over two-thirds are located to the left of the superior mesenteric artery [51].

Iso-vascular or hypovascular lesions are difficult to localize and may require additional imaging studies for lesion identification.

On MRI, insulinomas frequently show low signal intensity on T1-weighted fat-suppressed images and high signal intensity on T2-weighted images [52]. However, some tumors may be iso-intense to the pancreas on pre-contrast T1 sequences. Occasionally, an insulinoma can show low signal intensity on T2-weighted sequences due to the presence of a fibrous or sclero-hyaline stroma [52]. Diffusion-weighted sequences and the ADC map may help

in the identification of these tumors based on their high sensitivity and contrast resolution [42].

Most insulinomas show intense enhancement with gadolinium throughout the lesion, and some may demonstrate ring-like peripheral enhancement [53]. The presence of fibrous tissue diminishes the degree of enhancement during the early dynamic study and may be associated with delayed enhancement in some instances.

In conclusion, MDCT and MRI are the best imaging techniques for preoperatively diagnosing small pancreatic insulinomas, but in either case optimal technique and state-of-the-art equipment are mandatory. In cases in which CT, MRI, EUS, and scintigraphy results are negative, IOUS at the time of surgical resection represents the last opportunity to confirm these tumors in patients in whom strong clinical suspicion persists, and/or to find additional tumors. IOUS is particularly important in patients with multiple lesions and MEN1 since under these conditions ectopic tumors, which may be multiple, are quite frequent and difficult to find with CT or MRI [27].

9.6.2 Gastrinoma

Gastrinomas are usually larger than insulinomas at diagnosis (> 2 cm), multiple in 60% of patients, malignant in 60–65%, and associated with MEN1 in 20–60%.

Most of these tumors are located in the so-called gastrinoma triangle (between the junction of the head and neck of the pancreas, the second and third portion of the duodenum, the junction of the cystic duct and the common bile duct). Although gastrinomas are usually slow growing, approximately 50% of patients with gastrinoma have metastases at the time of diagnosis.

Gastrinomas are hypervascular tumors. They are best visualized by using thin-slice sections and a dual-phase CT protocol, with arterial and portal venous phases [54, 55]. The imaging technique is therefore similar to that used for other functioning tumors.

Due to their larger size, pancreatic gastrinomas are usually easily detected by MDCT; however, ectopically located tumors are more challenging.

Metastases to the liver and loco-regional lymph-nodes tend to be similar in appearance to the primary tumor [36].

MRI can also be employed for the identification and staging of gastrinomas, with some studies reporting sensitivities of 20–62% [54, 55].

EUS was shown to be cost-effective compared with a control group examined by venous sampling [56].

Results with angiography vary greatly across studies [54]. CT and MRI have the advantage of staging the entire abdomen and pelvis, which is not possible with the limited depth penetration of EUS. In equivocal or negative cases with a high clinical suspicion, somatostatin-receptor scintigraphy is very

effective in assessing both the primary tumor in the pancreas or ectopic sites and metastatic lesions to the liver.

9.6.3 VIPoma

On average, these tumors share similar imaging feature with other functioning endocrine tumors. VIPomas are usually > 3 cm in diameter at the time of diagnosis and may be malignant in over 60% of the cases [57, 58].

The majority of the neoplasms are located in the body or tail of the pancreas [58]. Occasionally, tumors causing a similar clinical syndrome are located in the adrenal glands, retroperitoneum, ganglia of sympathetic chain, lung, and as intestinal carcinoids [57, 58]. Rarely, these tumors are associated with MEN1 [59]. Statistical data concerning the accuracy of imaging studies are not available.

MDCT, MRI, US, and angiography have been used to localize the primary lesion and to identify metastases. On contrast-enhanced imaging studies, the latter, mainly involving the liver, frequently show intense enhancement similar to the appearance of the primary tumor.

9.6.4 Glucagonoma

Glucagonomas are intrapancreatic tumors mostly involving the head and neck of the gland.

They occur with a slight prevalence in women, with a peak age of 55 years [60]. The tumor is malignant in about 60% of patients, and the 5-year survival is 50%. When not diagnosed on the basis of clinical and laboratory findings, glucagonomas become symptomatic, causing symptoms related to mass effect, locoregional infiltration, and lymph node and liver metastases.

CT, MR, angiography, and US have been used successfully to diagnose and stage these tumors, but in all reports the conclusions were based only on anecdotal references [10, 61].

9.6.5 Somatostatinoma

Somatostatinomas are usually solitary, aggressive lesions occurring in the fourth to sixth decades of life. Metastases at the time of diagnosis have been described in more than 70% of patients in some series [62]. This tumor is usually located within the pancreas, where it tends to be quite large (2–10 cm in diameter); 75% occur in the head [51].

However, somatostatinomas may also arise within small bowel loops, the duodenal ampulla, or the peri-ampullary region [62].

A prevalence of duodenal locations for men and pancreatic locations for women has been described [63]. When the small bowel is involved, the neoplasm can be considered as a carcinoid that consists almost completely of somatostatin-containing cells but produces little somatostatin.

Extrapancreatic lesions, with a mean diameter of about 2 cm, are frequently diagnosed early because of the presence of symptoms such as jaundice, bleeding, and ulcerations.

The radiologic features of somatostatinomas resemble those of other neuroendocrine tumors.

Imaging studies usually demonstrate a hypervascular lesion, with or without hypervascular lymph nodes and liver metastases [64].

The demonstration of ectopically located tumors, involving the duodenum or intestinal loop, may be challenging for radiologists. In suspected cases, a dedicated protocol including filling of the duodenal and intestinal loops with water or oral contrast material may facilitate the detection of ectopically located primary tumors.

9.6.7 Other F-PanNENs

Other, very rare functioning endocrine tumors of the pancreas have been occasionally described, including corticotropinoma, ACTHoma, and GRFoma. Their clinical diagnosis is challenging because they are clinically not associated with a specific endocrine syndrome.

Like all the other functioning endocrine tumors, these rare neoplasms usually demonstrate the features of a hypervascular mass without or with liver metastases.

9.7 Diagnostic Strategies for F-PanNENs

Functioning endocrine tumors of the pancreas continue to challenge the radiologist. Earlier reports showed that up to 27% of patients have tumors not detected preoperatively with either helical CT or MRI. Sensitivities that approach 90–95% for lesions located in the pancreatic head region are achieved with EUS, but its sensitivity is limited for lesions located in the tail; also, EUS cannot be used for reliable preoperative staging.

Ectopically located, extra-pancreatic F-NENs are likewise imaged with difficulty, especially when they are small in diameter.

Overall, arteriography and venous sampling are no longer routinely employed even in difficult cases, because of the inherent technical problems associated with the test and the higher cost.

More recently, somatostatin-receptor scintigraphy and positron emission tomography have been used to establish or confirm the presence of ectopic

lesions or small masses suspected on CT or MRI, and to improve results in assessing metastatic disease.

The best results are reportedly obtained with a combination of intraoperative palpation and IOUS due to their complementary nature during surgery.

Somatostatin-receptor techniques can be used for treatment and to monitor its success in patients with functioning tumors of the pancreas [65].

9.8 Diagnostic Strategies for NF-PanNENs

In most cases, NF-PanNENs are found by chance in patients suffering from non-specific symptoms (palpable mass, dyspepsia, etc.). In these settings, the diagnosis is usually late, and either US or CT is the first method to suggest the diagnosis. With the recent increase in the number and quality of cross-sectional imaging studies, a significant percentage of these lesions are discovered incidentally in asymptomatic patients.

The role of the radiologist is to characterize the lesion, demonstrating the typical hypervascular enhancement pattern, using CT, MRI, or CEUS.

However, since a definite characterization is not objectively possible with imaging, fine-needle biopsy is always advisable before treatment.

The prognosis of patients with NF-PanNENs is much better than that of patients with ductal adenocarcinomas, and therefore a surgical attempt integrated with chemotherapy is indicated even in more advanced stages of the disease. Accurate staging of the tumor can be obtained with CT or MRI [13].

MDCT and MRI findings are virtually identical: but based on its wide availability and slightly higher accuracy in preoperative staging, the former should be considered as the imaging tool of choice [13].

Nuclear medicine could improve tumor staging, as it is able to identify distant metastases and to assess the potential benefits of treatment with somatostatin analogues, either cold or radiolabeled. The presence of somatostatin receptor subtype 2 is promising in terms of treatment success. Moreover, in the follow-up of these tumors, due to the further advantage of identifying distant metastases, nuclear medicine techniques may be advisable, given that CT and MRI are able to distinguish scar tissue from the residual or relapsing tumor only with difficulty, especially in operated patients.

9.9 Differential Diagnosis

The diagnosis of F-PanNENs usually does not pose any dilemmas. Problems that arise in the differential diagnosis between NF-PanNENs and the other pancreatic masses vary according to the radiological aspect of the tumor, which in turn is strictly dependent on its vascular behavior.

The most typical variant of NF-PanNENs, characterized by a solid hyper-

vascularized appearance at imaging, is usually easily diagnosed on CT, MRI, and CEUS due to its conspicuous enhancement after contrast medium administration. Characterization of these tumors is also facilitated by the presence of hypervascularized hepatic metastases.

Rare tumors that show a hypervascular enhancement pattern during the arterial pancreatic phase and potentially mimicking the solid variant of NF-PanNENs include acinar carcinoma [66] and serous cystadenoma, in their solid variant [67]. Ductal adenocarcinoma, in rare cases, exhibits strong enhancement, necessitating a differential diagnosis.

Finally, hypervascularized pancreatic metastases, especially from renal tumors, must be taken into account, since they may have the same pattern [68]. However, the differential diagnosis is simple if there is a known primary tumor and other synchronous or metachronous metastases.

Moreover, pancreatic metastases, which can appear many years after identification of the primary tumor, are frequently multiple.

The solid hypovascularized variant of NF-PanNEN cannot be reliably characterized using cross-sectional imaging, and biopsy is always needed. If an infiltrating growth pattern is depicted at imaging, with or without associated hypovascularized liver metastases, imaging will not allow the differential diagnosis with pancreatic adenocarcinoma.

When the tumor presents as an expansive growth pattern with well-defined contours, especially in young women, the differential diagnosis must include a solid pseudopapillary tumor.

Finally, rare cystic endocrine tumors cannot be differentiated on the basis of imaging findings from mucinous cystic tumors (especially unilocular lesions) or solid pseudopapillary tumors in their cystic variant.

An intrapancreatic accessory spleen should be considered in the differential diagnosis of F-NENs and NF-PanNENs. It can be ruled out based on differences in vascular behavior, or in some cases in signal intensity at baseline MRI.

References

1. Kaltsas GA, Besser GM, Grossman AB (2004) The diagnosis and medical management of advanced neuroendocrine tumors. Endocr Rev 25:458-511
2. Eriksson B, Oberg K (2000) Neuroendocrine tumours of the pancreas. Br J Surg 87:129-131
3. Lam KY, Lo CY (1997) Pancreatic endocrine tumour: a 22-year clinicopathological experience with morphological, immunohistochemical observation and a review of the literature. Eur J Surg Oncol 23:36-42
4. Hoff A, Cote G, Gagel R (2004) Management of neuroendocrine cancers of the gastrointestinal tract: islet cell carcinoma of the pancreas and other neuroendocrine carcinomas. In: Abbruzzese J, Evans D, Willett C, Fenoglio-Preiser C (eds.) Gastrointestinal oncology. Oxford University Press, New York, pp. 780-800
5. Solcia E, Capella C, Kloppel G (1997) Tumors of the pancreas, vol fasc 20. AFIP atlas of tumor pathology, 3rd edn. Armed Forces Institute of Pathology, Washington DC
6. Dixon E, Pasieka JL (2007) Funtioning and nonfuntioning neuroendocrine tumors of the pancreas. Curr Opin Oncol 19:30-35

7. Rockall AG, Reznek RH (2007) Imaging of neuroendocrine tumours (CT/RM/US). Best Pract Res Clin Endocrinol Metab 21:43-68
8. Modlin IM, Oberg K, Chung DC et al (2008) Gastroenteropancreatic neuroendocrine tumours. Lancet Oncol 9:61-72
9. Kloppel G, Heitz PU (1988) Pancreatic endocrine tumors. Pathol Res Pract 183:155-168
10. Phan GQ, Yeo CJ, Hruban RH et al (1998) Surgical experience with pancreatic and peripancreatic neuroendocrine tumors: review of 125 patients. J Gastrointest Surg 2:472-482
11. Falconi M, Bonora A, Bassi C et al (2000). In: Pederzoli P, Bassi C (eds) Pancreatic tumors. Achievement and prospective. Thieme, Struttugart, pp. 368-397
12. Falconi M, Bettini R, Boninsegna L et al (2006) Surgical strategy in the treatment of pancreatic neuroendocrine tumors. JOP 7:150-156
13. Foti G, Boninsegna L, Falconi M, Pozzi Mucelli R (2012) Preoperative assessment of nonfunctioning pancreatic endocrine tumors: role of MDCT and MRI. Rad Med (in press)
14. Solcia E, Kloppel G, Sobin L et al (2000) Histological typing of endocrine tumours. World Health Organization International Histological Classification of Tumours, 2nd edn. Springer, Berlin
15. Fugazzola C, Procacci C, Bergamo Andreis IA et al (1990) The contribution of ultrasonography and computed tomography in the diagnosis of nonfunctioning islet cell tumors of the pancreas. Gastrointest Radiol 15:139-44
16. Hessel SI, Siegelman SS, McNeil BI (1982) A prospective evaluation of computed tomography and ultrasound of the pancreas. Radiology 143:129-133
17. D'Onofrio M, Mansueto G, Vasori S (2003) Contrast enhanced ultrasonographic detection of small pancreatic insulinoma. J Ultrasound Med 22:4413-4417
18. D'Onofrio M, Zamboni G, Faccioli N et al (2007) Ultrasonography of the pancreas. Contrast-enhanced imaging. Abdominal Imaging 32:171-181
19. D'Onofrio M, Malagò R, Zamboni G et al (2005) Contrast-enhanced ultrasonography better identifies pancreatic tumor vascolarization than helical CT. Pancreatology 5:398-402
20. D'Onofrio M, Mansueto G, Falconi M et al (2004) Neuroendocrine pancreatic tumor: value of contrast enhanced ultrasonography. Abdom Imaging 29:246-258
21. Schumacher B, Liibke HI, Frieling T (1996) Prospective study on the detection of insulinomas by endoscopic ultrasonography. Endoscopy 28:273-276
22. Gress FG, Barawi M, Kim D, Grendell IH (2002) Preoperative localization of a neuroendocrine tumor of the pancreas with EUS-guided line needle tattooing. Gastrointest Endosc 55:594-597
23. Alsohaibani F, Bigam D, Kneteman N et al (2008) The impact of preoperative endoscopic ultrasound on the surgical management of pancreatic neuroendocrine tumours. Can J Gastroenterol 22:817-820
24. Gunther RW, Klose KI, Ruckert K et al (1985) Localization of small islet-cell tumors. Preoperative and intraoperative ultrasound, computed tomography, arteriography digital subtraction angiography, and pan-creatic venous sampling. Gastrointest Radiol 10:145-152
25. Malagò R, D'Onofrio M, Zamboni GA et al (2009). Contrast-enhanced sonography of nonfunctioning pancreatic neuroendocrine tumors. Am J Roentgenol 192:424-30
26. Hayakawa T, Iin CX, Hirooka Y (2000) Endoscopic ultrasonography of the pancreas: new advances. IOP 1:46-48
27. Lewis MA, Thompson GB, Young WF Jr (2012) Preoperative Assessment of the Pancreas in Multiple Endocrine Neoplasia Type 1. World J Surg [Epub ahead of print]
28. Procacci C, Carbognin G, Accordini S et al (2001) Nonfunctioning endocrine tumors of the pancreas: possibilities of spiral CT characterization. Eur Radiol 11:1175-1183
29. lglesias A, Arias M, Casal M et al (2001) Unusual presentation of a pancreatic insulinoma in helical CT and dynamic contrast-enhanced MR imaging: case report. Eur Radiol 11:926-930
30. Stafford Iohnson DB, Francis IR, Eckhauser FE et al (1998) Dual-phase helical CT of nonfunctioning islet cell tumors. Comput Assist Tomogr 22:59-63
31. Ichikawa T, Peterson MS, Federle MP et al (2000) lslet cell tumor of the pancreas: biphasic CT versus MR imaging in tumor detection. Radiology 216:163-171

32. McNulty NI, Francis 1R, Platt IF et al (2001) Multi-detector row helical CT of is pancreas: effect of contrast-enhanced multiphasic imaging on enhancement of the pancreas, peripancreatic vasculature and pancreatic adenocarcinoma. Radiology 220:97-102
33. Graziani R, Brandalise A, Bellotti M et al (2010). Imaging of neuroendocrine gastroenteropancreatic tumours. Radiol Med 115:1047-1064
34. Chung MI, Choi BI, Han IK et al (1997) Functioning islet cell tumor of the pancreas. Localization with dynamic spiral CT. Acta Radiol 38:135-138
35. Boninsegna L, Partelli S, D'Innocenzio MM et al (2010) Pancreatic cystic endocrine tumors: a different morphological entity associated with a less aggressive behavior. Neuroendocrinology 92:246-251
36. Debray MP, Geoffroy O, Laissy IP et al (2001) Imaging appearances of metastases from neuroendocrine tumours of the pancreas. Br I Radiol 74:1065-1070
37. Keogan MT, McDermott VG, Paulson EK et al (1997) Pancreatic malignancy: effect of dual-phase helical CT in tumor detection and vascular opacification. Radiology 205:513-518
38. Van Hoe L, Gryspeerdt S, Marchal G et al (1995) Helical CT for the preoperative localization of islet cell tumors of the pancreas: value of arterial and parenchymal phase images. Am J Roentgenol 165:1437-1439
39. Koito K, Namieno T, Nagakawa T, Morita K (1997) Delayed enhancement of islet cell carcinoma on dynamic computed tomography: a sign of its malignancy. Abdom Imaging 22:304-306
40. Kalra MK, Maher MM, Mueller PR et al (2003) State-of-the-art imaging of pancreatic neoplasms. Br J Radiol76:857-865
41. Sung ER, Seung EJ, Kang HL et al (2007) CT and MR imaging findings of endocrine tumor of the pancreas according to WHO classification. European Journal of Radiology 62 371–377
42. Caramella C, Dromain C, De Baere T et al (2010) Endocrine pancreatic tumours: which are the most useful MRI sequences? Eur Radiol 20:2618-27
43. Carlson B, Iohnson CD, Stephens DH et al (1993) MRI of pancreatic islet cell carcinoma. J Comput Assist Tomogr 17:735-740
44. Buetow PC, Miller DL, Parrino TV, Buck IL (1997) lslet cell tumors of the pancreas: clinical, radiologic, and pathologic correlation in diagnosis and localization. Radiographics 17:453-472
45. Owen NI, Sohaib SA, Peppercorn PD et al (2001) MRI of pancreatic neuroendocrine tumours. Br I Radiol 74:968-973
46. Lewis RB, Lattin GE, Paal E (2010). Pancreatic endocrine tumors: radiologicalclinicopathological correlation. Radiographics 30:1445-64
47. Petersein I, Spinazzi A, Giovagnoni A et al (2000) Focal liver lesions: evaluation of the efficacy of gadobenate dimeglumine in MR imaging - a multicenter phase III clinical study. Radiology 215:727-736
48. Motosugi U, Ichikawa T, Morisaka H et al (2011) Detection of Pancreatic Carcinoma and Liver Metastases with Gadoxetic Acid-enhanced MR Imaging: Comparison with contrast-enhanced multi-detector row CT. Radiology 260:446-453
49. Doppman IL, Nieman L, Miller DL et al (1989) Ectopic adrenocorticotropic hormone syndrome: localization studies in 28 patients. Radiology 172:115-124
50. Vinik A1, Moattari AR, Cho K, Thompson N (1990) Transhepatic portal vein catheterization for localization of sporadic and MEN gastrinomas: a ten-year experience. Surgery 107:246-255
51. Howard TI, Stabile BE, Zinner MI et al (1990) Anatomic distribution of pancreatic endocrine tumors. Am I Surg 159:258-264
52. Thoeni RF, Mueller-Lisse UG, Chan R et al (2001) Detection of small, functional islet cell tumors in the pancreas: selection of MRI Imaging sequences for optimal sensitivity. Radiology 214:483-490
53. Kraus BB, Ros PR (1994) Insulinoma: diagnosis with fat-suppressed MR imaging. AJR 162:69-70
54. Frucht H, Doppman IL, Norton IA et al (1989) Gastrinomas: comparison of MR imaging with CT, angiography, and US. Radiology 171:713-717

55. Pisegna IR, Doppman IL, Norton IA et al (1993) Prospective comparative study of the ability of MR imaging and other imaging modalities to localize tumors in patients with Zollinger-Ellison syndrome. Dig Dis Sci 38:1318-1328
56. Bansal R, Tierney W, Carpenter S et al (1999) Cost effectiveness of EUS for preoperative localization of pancreatic endocrine tumors. Gastrointest Endosc 49:19-25
57. Kloppel G, Heitz PU (1988) Pancreatic endocrine tumors Pathol Res Pract 183:155-168
58. Iaffe BM (1987) Surgery for gut hormone-producing tumors. Am I Med 82:68-76
59. Krejs GI (1987) V1Poma syndrome. Am I Med 82:37-48
60. Bloom SR, Polak IM (1987) Glucagonoma syndrome. Am J Med 82:25-36
61. Solivetti FM, Giunta S, Caterino M et al (2001) CT findings in a case of glucagonoma with necrolytic migrating erythema. Radiol Med (Torino) 102:410-412
62. Tanaka S, Yamasaki S, Matsushita H et al (2000) Duodenal somatostatinoma: a case report and review of 31 cases with special reference to the relationship between tumor size and metastasis. Pathol Int 50:146-152
63. Patel YC, Ganda OP, Benoit R (1983) Pancreatic somatostatinoma: abundance of somatostatin-28(1-12)-like immunoreactivity in tumor and plasma. I Clin Endocrinol Metab 57:1048-1053
64. Semelka RC, Custodio CM, Cem Balci N, Woosley IT (2000) Neuroendocrine tumors of the pancreas: spectrum of appearances on MRI. I Magn Reson Imaging 11:141-148
65. Ugur O, Kothari PI, Finn RD et al (2002) Ga-66 labeled somatostatin analogue DOTA-DPhe1-Tyr3-octreotide as a potential agent for positron emission tomography imaging and receptor mediated internal radiotherapy of somatostatin receptor positive tumors. Nucl Med Biol 29:147-157
66. Ogawa T, Isaji S, Yabana T (2000) A case of mixed acinar endocrine carcinoma of the pancreas discovered in an asymptomatic subject. Int I Pancreatol 27:249-257
67. Gabata T, Terayama N, Yamashiro M et al (2005) Solid serous cystadenoma of the pancreas: MR imaging with pathologic correlation. Abdom Imaging 30:605-609
68. Ghavamian R, Klein KA, Stephens DH et al (2000) Renal cell carcinoma metastatic to the pancreas: clinical and radiological features. Mayo Clin Proc 75:581-585